FINAL REPORT FOR AFOSR GRANT NUMBER F49620-01-1-0158 FOR THE PERIOD February 1, 2001 to December 31, 2004

AEROELASTICITY, AEROTHERMOELASTICITY AND AEROELASTIC SCALING OF HYPERSONIC VEHICLES

Principal Investigator:
Peretz P. Friedmann
François-Xavier Bagnoud Professor
Phone 734-763-2354; FAX 734-763-0578; Email peretzf@umich.edu
Co-Principal Investigator:
Kenneth G. Powell, Professor
Phone 734-764-3331; FAX 734-763-0578; Email powell@umich.edu
Department of Aerospace Engineering
The University of Michigan
1320 Beal Ave.
Ann Arbor, MI 48109-2140

Introduction and Problem Statement

In recent years, renewed activity in hypersonic flight research has been stimulated by the current need for a low cost, single-stage-to-orbit (SSTO) or two-stage-to-orbit (TSTO) reusable launch vehicle (RLV) and the long term design goal of incorporating air breathing propulsion devices in this class of vehicles. The X-33, an example of the former vehicle type, was a 1/2 scale, fully functional technology demonstrator for the full scale VentureStar. Another hypersonic vehicle research program completed in May of the current year was the NASA Hyper-X experimental vehicle effort. Other activities are focused on the design of unmanned hypersonic vehicles that meet the needs of the US Air Force. The present study is aimed at enhancing the fundamental understanding of the aeroelastic behavior of vehicles that belong to this category and operate in a typical hypersonic flight envelope.

Vehicles in this category are based on a lifting body design. However, stringent minimum-weight requirements imply a degree of fuselage flexibility. Aerodynamic surfaces, needed for control, are also flexible. Furthermore, to meet the requirement of a flight profile that spans the Mach number range from 0 to 15, the vehicle must withstand severe aerodynamic heating. These factors combine to produce unusual aerothermoelastic problems that have received only limited attention in the past. Furthermore, it is important to emphasize that testing of aeroelastically scaled wind tunnel models, a conventional practice in subsonic and supersonic flow, is not feasible in the hypersonic regime. Thus, the role of aerothermoelastic simulations is more important for this flight regime than in any other flight regime.

Previous studies in this area can be separated into several groups. The first group consists of studies focusing on panel flutter, which is a localized aeroelastic

problem representing a small portion of the skin on the surface of the hypersonic vehicle [1-6]. The second group of studies in this area was motivated by a previous hypersonic vehicle, namely the National Aerospace Plane (NASP). Representative studies in this category are Refs. [7-11]. The third group of studies is restricted to recent papers that deal with the newer hypersonic configurations such as the X-33 or the X-34 [12-14]. The primary emphasis in these studies was on using unsteady aerodynamic loads based on piston theory, and in one case [14], the Euler solution for the unsteady aerodynamic loads was also employed. However, no aeroelastic studies were conducted on determining the role of viscosity on aeroelastic stability by solving the complete Navier-Stokes equations when combined with a structural dynamic model for the hypersonic vehicle. Furthermore, the even more complicated problem of aerothermoelasticity has received inadequate attention.

From the studies on various hypersonic vehicles [7, 14-16], one can identify operating envelopes for each vehicle, which can be combined to provide a graphical representation of operating conditions for this class of vehicles, shown in Fig. 1 (***Note-All the figures are provided at the end of this report***). In two studies [17, 18], an aeroelastic analysis capability for generic hypersonic vehicles in the Mach number range $0.5<M<15$, using computational aeroelasticity, has been developed under the auspices of this grant. The computational tool consisted of the CFL3D code, developed by NASA Langley, combined with a finite element model of a generic hypersonic vehicle utilizing NASTRAN. Using a composite operational envelope obtained by combining the characteristics of several hypersonic vehicles the hypersonic computational capability was validated by applying it on a two-dimensional double wedge typical section in the Mach number range of $2.0 < M < 15$. Flutter boundaries were obtained using piston theory, as well as unsteady aerodynamic loads based on Euler and Navier Stokes solutions [17, 18].

The principal objectives of the studies carried out in the framework of the current grant are to develop a physical understanding and effective computational techniques for the aeroelastic behavior of a generic hypersonic vehicle in level flight, operating throughout its entire flight envelope. This requires consideration of the three principal flight regimes of this vehicle, namely, subsonic, transonic and hypersonic, with an emphasis on the hypersonic regime. Thus, the specific objectives of the proposed research are: (1) develop an aeroelastic stability analysis procedure for unrestrained hypersonic vehicles operating in the Mach number range, $0.5<M<15$; (2) conduct detailed trend studies to determine the blend of modeling, mesh refinement and complexity that is required for the various flight regions mentioned for simple two-dimensional and three-dimensional cases as well as a complete generic hypersonic vehicle; (3) determine the aero-thermoelastic behavior of the vehicle by combining the heat transfer problem that determine the time dependent temperature distributions on the surface of the vehicle with the aeroelastic analysis.

During the period of the grant we have made remarkable progress in our

research activity as described in Refs. 19 and 20, which contain very interesting results for both the low aspect ratio wing configuration as well as the complete hypersonic vehicle. These results are described in the results section of this annual progress report.

Computational Aeroelasticity Study Using an Euler/Navier-Stokes Aeroelastic Solver-Method of Solution

A key element in a computational aeroelasticity study is the coupling between the fluid and structural portions of the model. Various methods have been proposed for coupled fluid-structure analysis when a CFD solver is combined with a finite element structural model, such as deforming meshes [21], the multiple-field formulation [22] and the mixed Lagrangian-Eulerian formulation [23]. In the deforming mesh approach [21], the edges of each element are represented as springs, with stiffnesses inversely proportional to the length of the edge. Grid points on the outer boundary of the mesh are held fixed, and the instantaneous locations of points on the inner boundary (body) are prescribed. In this study, the coupling of the fluid and the structure is done using a deforming mesh technique. In the multiple-field approach [22], the moving mesh is viewed as a psuedostructural system with its own dynamics and thus the coupled transient aeroelastic problem is formulated as a three-field problem: the fluid, the structure and the dynamic mesh. In the Mixed Lagrangian-Eulerian method [23], the governing equations for both the fluid and the structure are formulated in integral conservation form based on the same Lagrangian-Eulerian description. The entire fluid-structure continuum is treated as one continuum dynamics problem, while allowing for different discretization in the two domains. *In this study, the coupling of the fluid and the structure is done using a deforming mesh technique.*

An overview of the solution of the computational aeroelasticity problem in this study is shown in Fig. 2. First, the vehicle geometry is created using CAD software, and from this geometry a mesh generator is used to create a structured mesh for the flow domain around the body. In parallel, an unstructured mesh is created for the finite element model of the structure. Subsequently, the fluid mesh is used to compute the flow around the rigid body using the CFL3D code [24], while the structural mesh is used to obtain the free vibration modes of the structure by finite element analysis. The CFL3D code uses an implicit, finite-volume algorithm based on upwind-biased spatial differencing to solve the time-dependent Euler and Reynolds-averaged Navier-Stokes equations. For applications utilizing the thin-layer Navier-Stokes equations, the Spalart-Allmaras turbulence model is used. For an aeroelastic simulation, an additional term arising from the deforming mesh is included in the time-discretization of the governing equations. The aeroelastic equations are written in terms of a linear state-space equation and a modified state-transition-matrix integrator is used to march the coupled fluid-structural system forward in time, where the fluid forces are coupled with the structural equations of motion through the generalized aerodynamic forces. Using the flow solution as an initial condition, and the frequencies and mode shapes of the structure, an aeroelastic steady state is

obtained. Next, the structure is perturbed in one or more of its modes by an initial modal velocity condition, and the transient response of the structure is obtained. To determine the flutter conditions at a given altitude, aeroelastic transients are computed at several Mach numbers. The frequency and damping characteristics of the transient response at each Mach number can be determined from a moving block approach [25], and the flutter Mach number associated with this altitude can be estimated by interpolation.

Computational Model of the Double Wedge Airfoil and Low Aspect-Ratio Wing

A typical cross-section based on the double wedge airfoil, shown in Figs. 3 and 4, is a simple configuration for which aeroelastic stability and response results are generated independently using third order piston theory. The derivation of the piston theory model is given in Ref. [17. Results for this configuration using Euler and Navier-Stokes unsteady aerodynamic loads were generated and compared with the results from piston theory aerodynamics computations for the typical section analysis are carried out using a 225×65 C-grid with 225 points around the wing and its wake (145 points wrapped around the airfoil itself), and 65 points extending radially outward from the airfoil surface. The computational domain extends one chord-length upstream and six chord-lengths downstream, and one chord-length to the upper and lower boundaries. The double wedge airfoil and a portion of the surrounding computational grid are shown in Fig. 3.

In addition to the typical section analysis, a model for a low aspect-ratio wing has been created to study the aeroelastic behavior of control surfaces typical of reusable launch vehicles. The model, shown in Figs. 5 and 6, resembles the low aspect ratio wing of the Lockheed F-104 Starfighter. The natural frequencies and modes (Fig. 7) were determined by matching the fundamental bending and torsional frequencies and total mass of the model to the F-104 wing. The Euler and Navier-Stokes computations for the low aspect ratio wing are carried out using a 65x193x41 C-H grid with 193 points around the wing and its wake (97 points wrapped around the wing), 65 points extending spanwise from the root (25 points on the wing), and 41 points extending radially outward from the surface. The computational domain extends one root chord-length upstream, two root chord-lengths downstream, two semi-span lengths in the spanwise direction, and one-half root chord-length to the upper and lower boundaries. The wing and a portion of the surrounding computational grid are shown in Fig. 5. For the Navier-Stokes simulations, both the typical section and wing analyses use the Spalart-Allmaras turbulence model, along with an adiabatic wall temperature condition.

Results and Discussion

Aeroelastic Behavior of the Double Wedge Airfoil and Low Aspect-Ratio Wing

Aeroelastic response calculations for the double wedge typical section were carried out at an altitude of 40,000 and 50,000 feet at zero angle of attack. Numerous results were presented in Ref. 17 and 18. It was found that substantial differences (up to 20%) can be obtained between piston theory and Euler solutions. However, both Euler and Navier-Stokes aerodynamics predicts similar

aeroelastic behavior. The two-dimensional typical section was also useful for conducting careful mesh convergence studies from which the appropriate mesh size for this class of hypersonic computational aeroelastic problems could be determined. Large differences in aeroelastic stability boundaries between first order and third order piston theory were obtained for the typical section as indicated in Ref. 20, and therefore the use of first order piston theory for this class of problems is not recommended.

For the low aspect-ratio wing, the sensitivity of the aeroelastic behavior to the number of modes was studied and it was found that for converged results at least five elastic modes are required. In Refs. 19, 21 and 22 detailed and careful computational mesh convergence studies were carried out to determine the mesh that is most effective from a computational point of view when the calculation of the aerodynamic loads is based on the Euler equations. It was found that certain optimal meshes for the Euler calculations could be also used for Navier-Stokes based simulations. Results obtained for this configuration are presented in Figs. 8-11. Figure 8 depicts the damping and frequencies obtained from the moving block analysis for the 5 aeroelastic modal responses of the low aspect ratio wing using 3rd piston theory; the flutter boundary is found to be at M_f = 13.5. Figure 9 shows the same information for the case when the unsteady loads are based on Euler aerodynamics, for this case flutter occurs at M_f = 13.6. Figure 10 presents preliminary results based on using Navier-Stokes aerodynamics in this case M_f= 13.52. These results show that, for this configuration and altitude, the flutter Mach number is not significantly affected when the various aerodynamic methods are used. These results also indicate that for the low aspect ratio wing at this altitude, viscosity may not play an important role. The typical reduced frequency range for these cases was low, which explains the relatively small differences between third order piston theory, Euler based unsteady loading and solutions based on the Navier Stokes equations.

References 21 and 22 also contain a careful study of three methods for identifying the damping and the frequency of an aeroelastic system from its transient time response history were carefully examined for the hypersonic aeroelastic problem. The three methods considered were: (1) moving block approach (MBA) [27], (2) least squares curve fitting method (LSCFM) [28], and the Auto-Regressive-Moving Average (ARMA) model [29,30]. It was found that all three methods were capable of identifying damping and frequency in a reliable method. However, the reliability of the identification process was dependent on the length of the time record for which the response of the aeroelastic system is given. When comparing the three methods it turns out that the ARMA model is the most reliable and what is most important it requires a time record that is only 25% in length when compared to the time record needed for identification for the other two approaches. This has very significant implications in computational aeroelasticity since it reduces by 75% the computer time required to identify a flutter boundary. Therefore, this is the method of choice for cases involving time-consuming computation using the Navier Stokes or Euler equations.

Aerothermoelastic Behavior of the Low Aspect-Ratio Wing

Preliminary results, presented in Ref. [19], based on a simple aerothermoelastic model of the low aspect ratio wing, with a *prescribed temperature distribution*, indicate that the presence of non-uniform aerodynamic heating can substantially alter the frequencies and modes of the structure due to change in effective material stiffness and thermal stresses. For this particular case, two areas of instability manifest themselves as illustrated in Fig. 11. The first instability occurs at M = 5.25, where the structure becomes unstable as a result of thermal buckling; another (somewhat contrived) instability occurs at M = 9.0. In Ref. [19], the non-uniform temperature distribution used in these calculations was assumed to exist throughout the wing.

A concise review of the limited research that has been done in the area of aerothermoelasticity is provided in Refs. 21 and 22. Reference 21 is attached as Appendix A of this report for the sake of completeness. The low aspect ratio wing considered in this study is built of aluminum. Such a wing needs a thermal protection system (TPS) so as to be able to withstand the harsh thermal environment that exists in hypersonic flow. It is assumed that such a thermal protection system exists on the wing, so that it can withstand temperatures of up to 1500° K, while the supporting structure operates at temperatures that can be tolerated by aluminum.

Exact treatment of aerothermoelasticity requires coupling of the unsteady heat transfer problem with the aeroelastic problem based on the Navier-Stokes solution of the unsteady airloads, which results in dependent temperature distributions. This implies time dependent free vibration characteristics of the structure, at a given Mach number, as it is heated. The heat transfer between the fluid and the structure, schematically depicted in Fig. 12 is determined from an energy balance of the heat fluxes at the wall of the structure. The heat transfer represents the balance at the wall between convective heating of the fluid ($\dot{q}_{aero}$) and heat loss due to conduction in the structure ($\dot{q}_{cond}$), radiation out to space ($\dot{q}_{rad}$) and energy stored in the wall ($\dot{q}_{strd}$). The details of this solution are provided in Ref. 21. The aerodynamic heating is obtained from rigid body CFD computations. This is subsequently introduced in the finite element analysis of the structural system. The transient temperature distribution in the structure is determined from a finite element based heat transfer analysis (available in NASTRAN). Subsequently the free vibration mode shapes and frequencies of the transiently heated structure are calculated at each desired point in time and used in the aeroelastic analysis. Note that this is not an exact treatment of the aerothermoelastic system, since the temperature distribution is not computed at each time step of the aeroelastic calculation. However, this assumption is quite reasonable since the heat loads very slowly with time when compared to the generalized forces and motions of the aeroelastic system.

To gain insight into the effect of aerodynamic heating on the flutter boundary, the heated mode shapes of the wing were used to calculate the flutter boundary at 100,000 ft using third order piston theory. The flutter boundaries of the heated and cold wing are compared in Fig. 13. Both NASP and X-43 ascent

trajectories are depicted. Newtonian impact aerodynamics are also used for comparison since the Mach numbers are high. The important result shown in Fig. 13 is the reduction in the flutter velocity for the heated wig, with a 2-degree angle of attack, to M_f=23.8 from its initial value of M_f=62.6, when cold. Clearly, careful treatment of the coupled heat transfer-aeroelastic problem is critical in hypersonic vehicles.

Aeroelastic Behavior of a Generic Reusable Launch Vehicle

The model employed is based on a generic vehicle that resembles a potential reusable launch vehicle. The model represents the fuselage of the vehicle and canted fins, shown in Fig. 14. The dimensions of the generic vehicle are 76.2 ft. length, 45.54 ft. width, and 6 ft. thickness. The canted fins have a span of 18 ft. with a taper ratio of 0.25. They have double-wedge cross-sections with the maximum thickness at midchord, equal to 3.33% of the chord. The empty mass of the vehicle is considered to be 70,000 lbs. A modal convergence study was conducted for this configuration and it was found that 12 modes are required in order to obtain a converged solution. When using Euler aerodynamics, the results the flutter boundary is increased to M_f =9.3, which is 31% higher than that predicted by nonlinear piston theory. The significant difference in flutter boundaries predicted using the two aerodynamic models is due to the presence of three-dimensional flow effects. Prior to calculating the aeroelastic transients, the equilibrium state of the flexible vehicle was calculated by allowing the vehicle to deform in hypersonic flow, with the addition of artificial structural damping, to accelerate convergence. Since piston theory is a sectional theory, and each cross-section of the vehicle is symmetrical about the horizontal plane, the equilibrium state of the flexible vehicle is the same as the undeformed geometry. However, Euler aerodynamics introduces the effects of three-dimensional flow, which causes the fins to flatten out in the span-wise direction; which causes the typical cross-section to translate downward by nearly 1 foot, and it also undergoes significant deformation from the initial double-wedge shape.

A summary of these results is shown in Table 1 below, which also shows that 12 modes are required for a converged solution.

Table 1: Comparison of flutter boundaries for the generic vehicle, obtained using different models for predicting aerodynamic loads.

Model for aerodynamic loads	M_f, 7 modes	M_f, 12 modes
Piston theory, 1st order	16.2	13.2
Piston theory, 3rd order	11.7	7.2
Euler, coarse mesh	11.6	9.3
Euler, refined mesh	11.2	9.3

Very large differences in M_f – flutter Mach number are evident between 1st and 3rd order piston theory. For the 12-mode solution there are very substantial differences between piston theory and the Euler solution, however these differences are not evident in the 7-mode solution. This implies that approximate solutions can be unreliable, and design of a hypersonic vehicle has to be based on refined aeroelastic models.

The flutter envelope for a generic hypersonic vehicle, calculated using 12 modes is shown in Fig. 15. This figure compares flutter boundaries at various altitudes calculated using 3rd order piston theory and Euler aerodynamics on both coarse and refined meshes. At low altitudes, nonlinear piston theory predicts the flutter boundaries comparable to Euler aerodynamics based methods. However, at altitudes above 30,000 ft there is significant difference. The differences shown in Fig. 15 are magnified in Fig. 16 where dynamic pressures are compared. As evident, at higher altitudes piston theory under predicts the flutter dynamic pressure compared to Euler aerodynamics by 25-50%.

Concluding Remarks and Accomplishments

Since testing of aeroelastically scaled wind tunnel models is not feasible in the hypersonic regime, the role of aerothermoelastic simulations is critical. It should be also noted that the results obtained in the course of this research provide a validation of the CFL3D code for the hypersonic flight regime. The principal findings are summarized below.

- In general, the three-time domain frequency and damping identification techniques produce similar estimates of the aeroelastic behavior of a system. The ARMA method was superior, however, to both the LSCFM and MBA method since it provided quick damping and frequency estimates with minimal response record length. This is an important consideration because the length of response record required for accurate computation of system damping largely determines the cost of computational aeroelastic simulations. In this case, the ARMA method offers a 75% reduction in computational cost over the MBA.
- The aeroelastic behavior of a system, predicted using time-accurate CFD solutions of the Euler equations are sensitive to the number of sub-iterations used, as well as $CFL\tau$. Studies must be carried out on a case-by-case basis in order to ensure that these parameters have appropriate values.
- The aeroelastic behavior of the three-dimensional low aspect ratio wing obtained using piston theory, Euler and Navier-Stokes aerodynamics is similar. The flutter boundary obtained using Euler aerodynamics is approximately 2\% higher than that predicted by piston theory, while the flutter boundary obtained using Navier-Stokes aerodynamics is less than 1\% lower than the Euler solution.
- The presence of aerodynamic heating on a low aspect ratio cantilever structure, such as a fin and/or control surface on a hypersonic vehicle, will result in thermal stresses due to warping restraint at the root. This, combined with material property degradation, dramatically affects the natural

frequencies of the structure. Increasing the Mach number decreases the time before thermal buckling occurs. However, changes in frequency are similar for various Mach numbers when plotted as a function of leading edge temperature.

- Angle of attack is an important consideration when performing aerothermoelastic analysis of a structure, since it introduces additional thermal stresses that significantly degrade the stiffness of the structure for a given reference temperature, or point in time. Aerodynamic heating in this case has a substantial effect on the aeroelastic behavior of the low aspect ratio wing, reducing the flutter boundary by 62\%.
- For the generic vehicle, the aeroelastic model based on Euler solutions predicts a flutter boundary 31\% higher than that predicted by third-order piston theory, due to the presence of significant three-dimensional flow effects captured by Euler aerodynamics. This leads to significant deformation of the canted fins, and these two aerodynamic models predict different equilibrium configurations for the flexible vehicle. Hence, the surface pressure distributions are also found to be different. Since the aeroelastic transient solutions are calculated by considering small perturbations about these

Finally, it is important to note that Ref. 19, was picked as the best paper given at the 44th AIAA/ASME/ASCE/AHS/ASC Structures, Structural Dynamics and Materials Conference held in April 2003 in Norfolk, VA from a total of 526 papers presented at the conference. The authors (B. Thuruthimattam, P. Friedmann, J. McNamara and K. Powell) received the ASME/Boeing Structures and Materials award at the award luncheon of the 45th AIAA/ASME/ASCE/ AHS/ASC Structures, Structural Dynamics and Materials Conference held in Palm Springs, CA in April 2004. This is a strong testimony to the quality of the research carried out under the auspices of this AFOSR grant.

References

[1] Xue, D.Y. and Mei, C., "Finite Element Two-Dimensional Panel Flutter at High Supersonic Speeds and Elevated Temperature," AIAA Paper No. 90-0982, *Proc. 31st AIAA/ASME/ASCE/AHS/ASC Structures, Structural Dynamics and Materials Conference,* 1990, pp. 1464—1475.

[2] Gray, E.G. and Mei, C., "Large-Amplitude Finite Element Flutter Analysis of Composite Panels in Hypersonic Flow," AIAA Paper No. 92-2130, *Proc. 33rd AIAA/ASME/ASCE/ AHS/ASC Structures, Structural Dynamics and Materials Conference,* 1992, pp. 492—512.

[3] Abbas, J.F. and Ibrahim, R.A., "Nonlinear Flutter of Orthotropic Composite Panel Under Aerodynamic Heating," *AIAA J.,* Vol. 31, No. 8, No. 8, 1993, pp. 1478—1488.

[4] Bein, T., Friedmann, P., Zhong, X., and Nydick, I., "Hypersonic Flutter of a Curved Shallow Panel with Aerodynamic Heating," AIAA Paper No. 93-1318, *Proc. 34th AIAA/ASME/ASCE/AHS/ASC Structures, Structural Dynamics and Materials Conference,* 1993.

[5] Nydick, I., Friedmann, P.P. and Zhong, X., "Hypersonic Panel Flutter Studies on Curved Panels;' AIAA Paper No. 95-1485, *Proc. 36th AIAA/ASME/ASCE/AHS/ASC Structures, Structural Dynamics and Materials Conference,* 1995, pp. 2995-3011.

[6] Mei, C., Abdel-Motagly, K., and Chen, R., "Review of Nonlinear Panel Flutter at Supersonic and Hypersonic Speeds," *Applied Mechanics Reviews,* 1998.

[7] Ricketts, R., Noll, T., Whitlow, W., and Huttsell, L., "An Overview of Aeroelasticity Studies for the National Aerospace Plane," AIAA Paper No. 93-1313, *Proc. 34th AIAA/ASME/ASCE/AHS/ASC Structures, Structural Dynamics and Materials Conference,* 1993, pp. 152— 162.

[8] Scott, R.C. and Pototzky, A.S., "A Method of Predicting Quasi-Steady Aerodynamics for Flutter Analysis of High Speed Vehicles Using Steady CFD Calculations;' AIAA Paper No. 93-1364, *Proc. 34th AIAA/ASME/ASCE/AHS/ASC Structures, Structural Dynamics and Materials Conference,* 1993, pp. 595—603.

[9] Spain, C., Zeiler, T.A., Bullock, E., and Hodge, J.S., "A Flutter Investigation of All-Moveable NASP-Like Wings at Hypersonic Speeds," AIAA Paper No. 93-1315, *Proc. 34th AIAA/ASME/ASCE/AHS/ASC Structures, Structural Dynamics and Materials Conference,* 1993.

[10] Spain, C., Zeiler, T.A., Gibbons, M.D., Soistmann, D.L., Pozefsky, P., DeJesus, R.O., and Brannon, C.P., "Aeroelastic Character of a National Aerospace Plane Demonstrator Concept," *Proc. 34th AIAA/ASME/ASCE/AHS/ASC Structures, Structural Dynamics and Materials Conference,* 1993, pp. 163—170.

[11] Heeg, J., Zeiler, T., Pototzky, A., Spain, C., and Engelund, W., "Aerothermoelastic Analysis of a NASP Demonstrator Model," AIAA Paper No. 93-1366, *Proc. 34th AIAA/ASME/ASCE/AHS/ASC Structures, Structural Dynamics and Materials Conference,* 1993, pp. 617—627.

[12] Blades, E., Ruth, M., and Fuhrman, D., "Aeroelastic Analysis of the X-34 Launch Vehicle," AIAA Paper No. 99-1352, *Proc. 40th AIAA/ASME/ASCE/AHS/ASC Structures, Structural Dynamics and Materials Conference,* 1999, pp. 1321—1331.

[13] Nydick, I. and Friedmann, P.P., "Aeroelastic Analysis of a Generic Hypersonic Vehicle," NASA/CP-1999-209136/PT2, *Proc. CEAS/AIAA/ICASE/NASA Langley International Forum on Aeroelasticity and Structural Dynamics,* 1999, pp. 777— 810.

[14] Gupta, K.K., Voelker, L.S., Bach, C., Doyle, T., and Hahn, E., "CFD-Based Aeroelastic Analysis of the X-43 Hypersonic Flight Vehicle," AIAA Paper No. 2001-0712, *39th Aerospace Sciences Meeting & Exhibit,* 2001.

[15] Berry, SA., Horvath, T.J., Hollis, B.R., Thompson, R.A., and Hamilton, H.H., "X-33 Hypersonic Boundary Layer Transition," AIAA Paper No. 99-3560, *33rd AIAA Thermophysics Conference,* 1999.

[16] Riley, C.J., Kleb, W.L., and Alter, S.J., "Aeroheating Predictions for X-34 Using An Inviscid-Boundary Layer Method," AIAA 98-0880, *36th Aerospace Sciences Meeting & Exhibit,* 1998.

[17] Thuruthimattam, B.J., Friedmann, P.P, McNamara, J.J., and Powell, K.G., "Aeroelasticity of a Generic Hypersonic Vehicle," AIAA Paper No. 2002-1209, *Proc. 43rd AIAA/ASME/ASCE /AHS Structures, Structural Dynamics and Materials Conference,* 2002.

[18] Thuruthimattam, B.J., Friedmann, P.P, McNamara, J.J., and Powell, K.G, "Modeling Approaches to Hypersonic Aerothermoelasticity with Application to Reusable Launch Vehicles," AIAA Paper No. 2003-1967, *Proc. 44th AIAA/ASME/ASCE/AHS Structures, Structural Dynamics and Materials Conference,* 2003.

[19] McNamara, J. J., Thuruthimattam, B. J., Friedmann, P. P., Powell, K. G. and Bartels, R., "Hypersonic Aerothermoelastic Studies for Reusable Launch Vehicles," AIAA Paper 2004 - 1590, *Proceedings of the 45th AIAA/ASME/ ASCE/AHS/ASC Structures, Structural Dynamics and Materials Conference*, Palm Springs, CA, April 19-22, 2004, pp. 1-35.

[20] Friedmann, P. P, McNamara, J. J., Thuruthimattam, B. J and Nydick, I., "Aeroelastic Analysis of Hypersonic Vehicles," Journal of Fluids and Structures, Vol. 19, June 2004, pp 681-712.

[21] McNamara, J. J., Friedmann, P. P., Powell, K. G., Thuruthimattam, B. J. and Bartels, R., "Aeroelastic and Aerothermoelastic Vehicle Behavior In Hypersonic Flow," AIAA Paper 2005-2175, Proceedings of the 46th AIAA/ASME/ASCE/AHS/ASC Structures, Structural Dynamics and Materials Conference, Austin TX, April 18-21, 2005, pp. 1-48.

[22] McNamara, J. J., Friedmann, P. P., Powell, K. G., Thuruthimattam, B. J. and Bartels, R., "Three-Dimensional Aeroelastic and Aerothermoelastic Behavior In Hypersonic Flow," AIAA Paper 2005-3305, 13th AIAA/CIRA International Space Planes and Hypersonic Systems and Technologies Conference, Centro Italiano Richerche Aerospaziali (CIRA), May 16-20, 2005, Capua, Italy.

[23] Robinson, B.A., Batina, J.T., and Yang, H.T., "Aeroelastic Analysis of Wings Using the Euler Equations with a Deforming Mesh," *Journal of Aircraft,* Vol. 28, 1991, pp. 778—788.

[24] Farhat, C., Lesoinne, M., and Maman, N., "Mixed Explicit/Implicit Time Integration of Coupled Aeroelastic Problems: Three-Field Formulation, Geometric Conservation and Distributed Solution," *International Journal for Numerical Methods in Fluids*, Vol. 21, 1995, pp. 807—835.

[25] Bendiksen, O.O., "A New Approach to Computational Aeroelasticity," *Proceedings of the AIAA/ASME/ASCE/AHS/ASC 32nd Structure, Structural Dynamics and Materials Conference,* Baltimore, MD, April 8-9 1991, pp. 1712—1727.

[26] Krist, S.L., Biedron, R.T., and Rumsey, CL., "CFL3D User's Manual (Version 5.0)," NASA, TM 1998-208444, 1997.

[27] Bousman, W.G. and Winkler, D.J., "Application of the Moving-Block Analysis" AIAA 81-0653, *Proceedings of the AIAA Dynamics Specialist Conference,* 1981, pp. 755-763.

[28] Bennett, R. G. and Desmarais, R., "Curve Fitting of Aeroelastic Transient Response Data with Exponential Functions," NASA-SP-415, October 1975, pp. 43-58.

[29] Matsuzaki, Y. and Ando, Y., "Estimation of Flutter Boundary from Random Response due to Turbulence at Subcritical Speeds," *Journal of Aircraft*, Vol. 18, No. 10, 1981, pp. 862-868.

[30] Pak, C. G. and Friedmann, P. P., "New Time Domain Technique for Flutter Boundary Identification," *Proceedings of the AIAA Dynamics Specialists Conference*, AIAA Paper No 92-2102, Dallas, TX, April 1992, pp. 201-214..

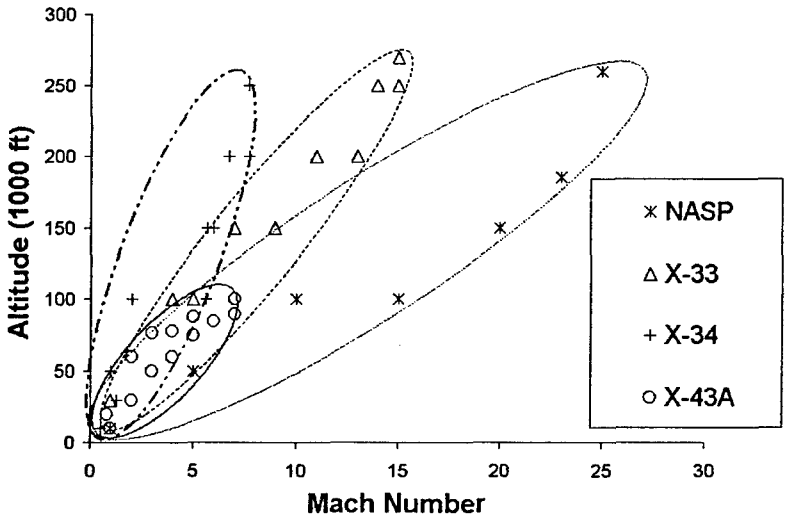

Figure 1: Operating envelopes for several modern hypersonic vehicles.

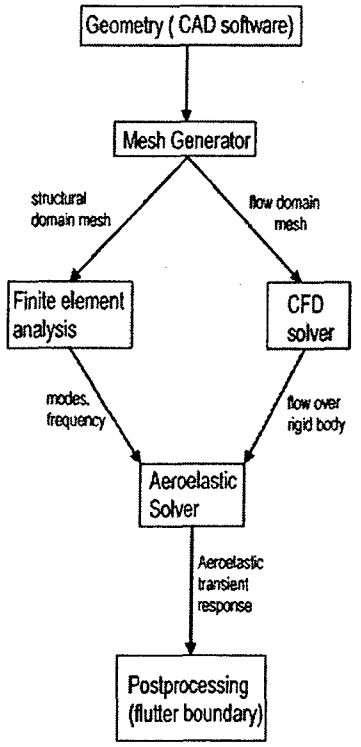

Figure 2: A flow diagram of the computational aeroelastic solution procedure.

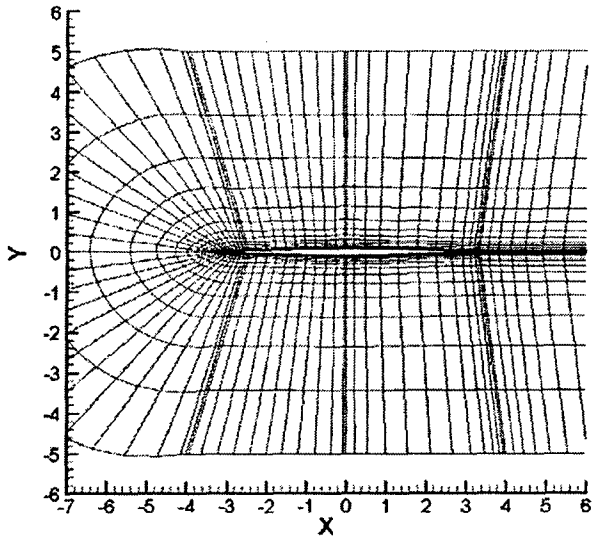

Figure 3: Diamond shaped airfoil section, and surrounding grid, to scale.

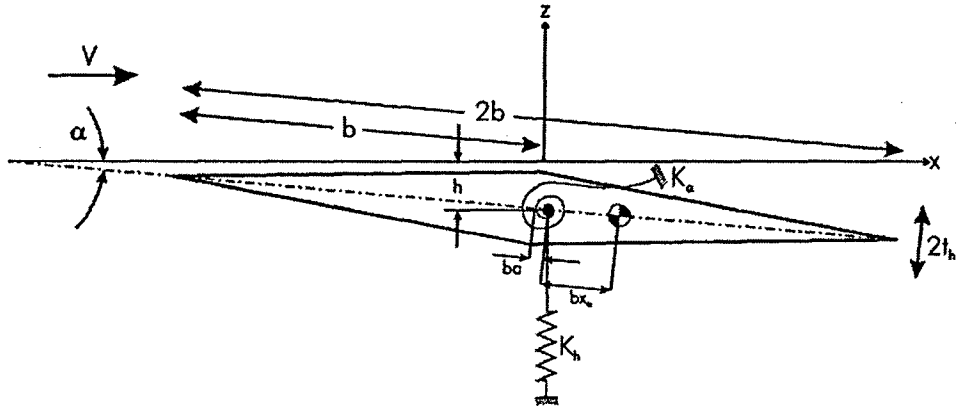

Figure 4: Two degree-of-freedom typical section geometry.

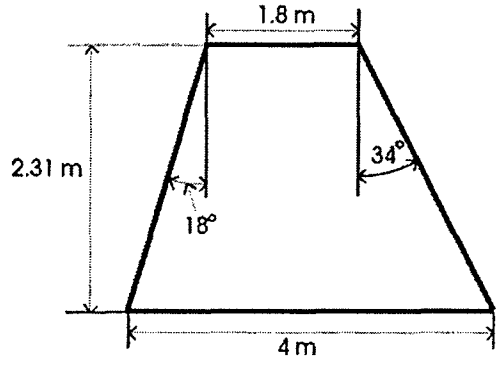

(a) Planform of the low aspect-ratio wing.

(b) Cross-sectional dimensions of low aspect-ratio wing.

Figure 5. A planform view of the low aspect-ratio wing, and a view of its cross-section.

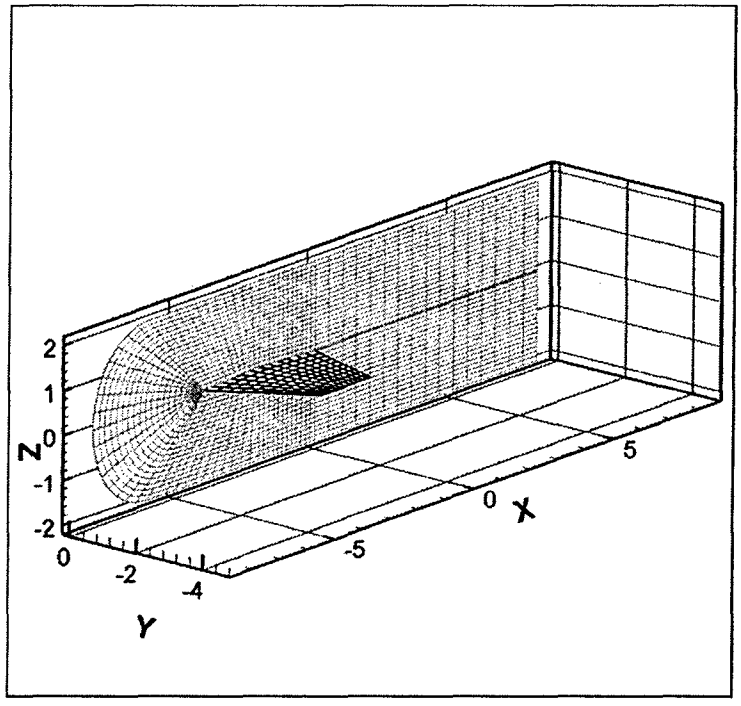

Figure 6. A coarsened view of the low aspect-ratio wing and its computational grid.

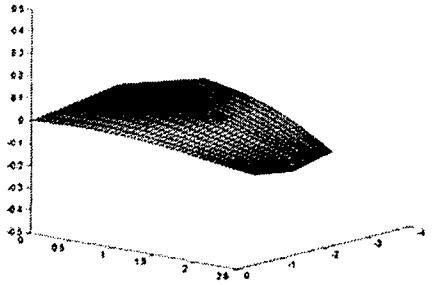

(a) Mode 1, 13.41 Hz. First bending mode.

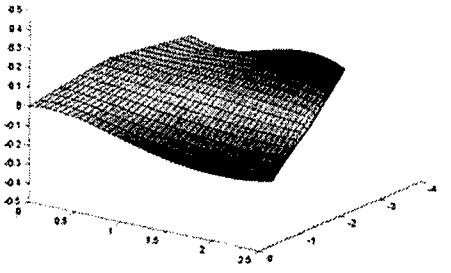

(b) Mode 2, 37.51 Hz. First torsional mode.

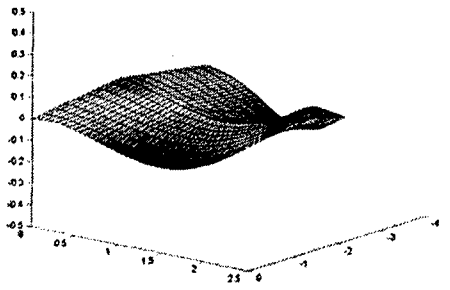

(c) Mode 3, 49.18 Hz. Second bending mode.

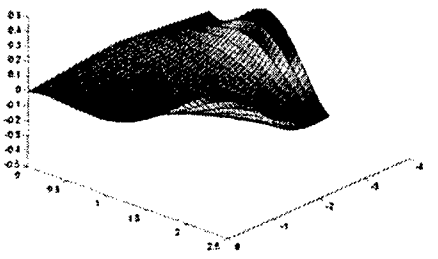

(d) Mode 4, 77.14 Hz. Second torsional mode.

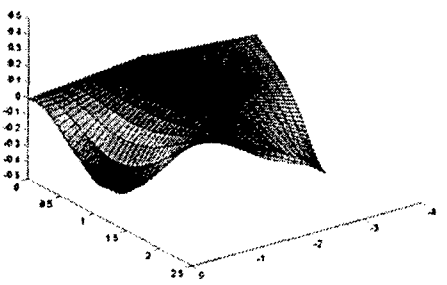

(e) Mode 5, 79.48 Hz.

Figure 7. First 5 free vibration modes of the low aspect-ratio wing.

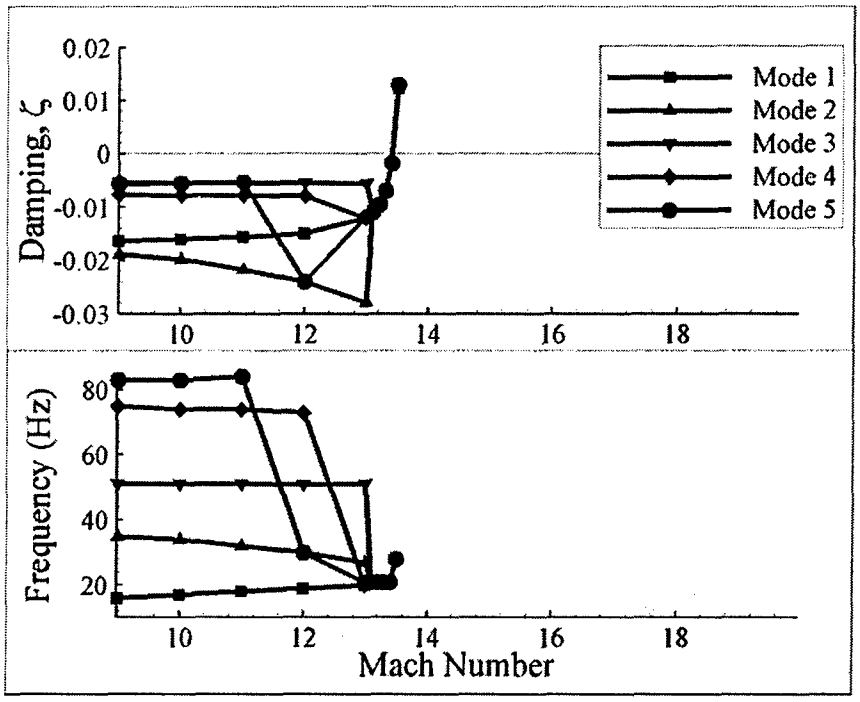

Figure 8: Aeroelastic behavior of the low aspect ratio wing using 3rd order piston theory aerodynamics. 40,000ft

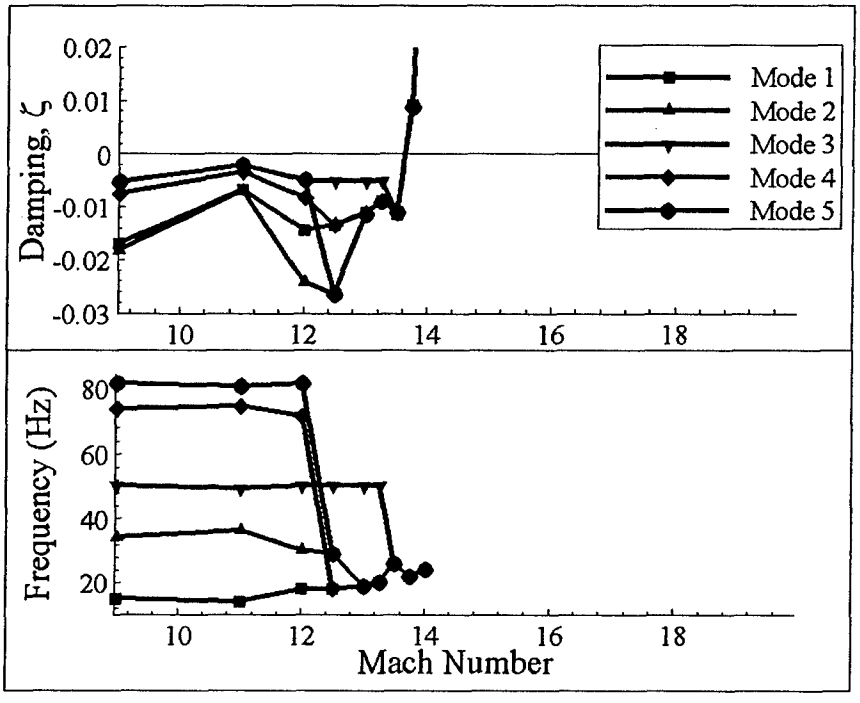

Figure 9: Aeroelastic behavior of the low aspect ratio wing using Euler aerodynamics. 40,000ft

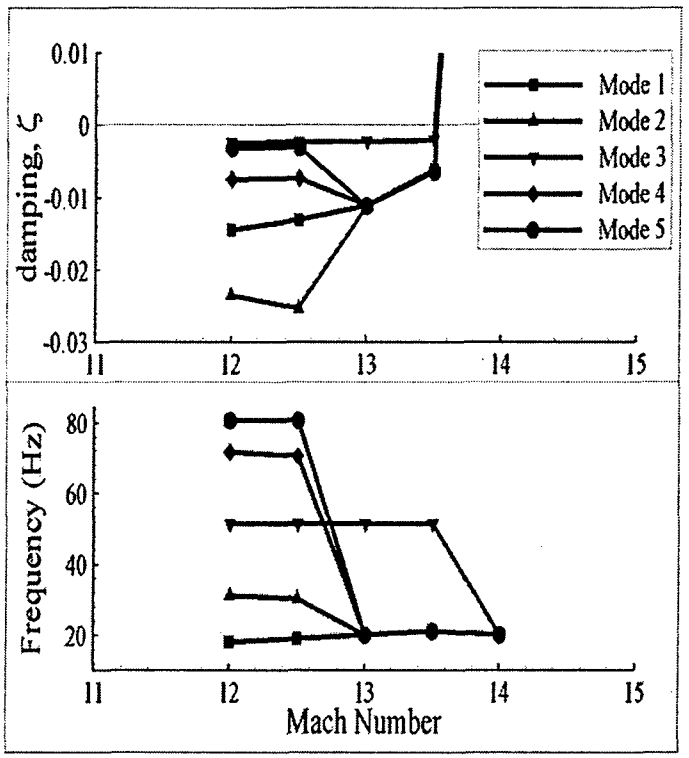

Figure 10: Aeroelastic behavior of the low aspect ratio wing using Navier-Stokes aerodynamics. 40,000ft

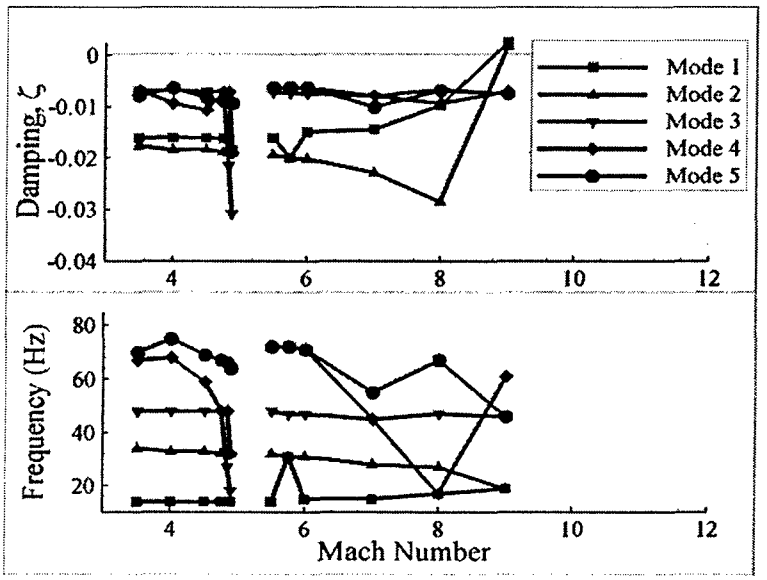

Figure 11: Aerothermoelastic behavior of the low aspect ratio wing subject to non-uniform heating using 3rd order piston theory aerodynamics. 40,000ft

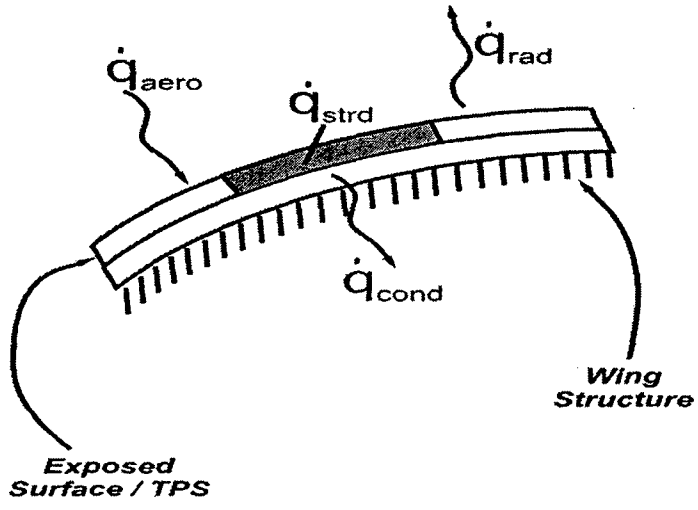

Figure 12: Heat Transfer at wall of hypersonic vehicle

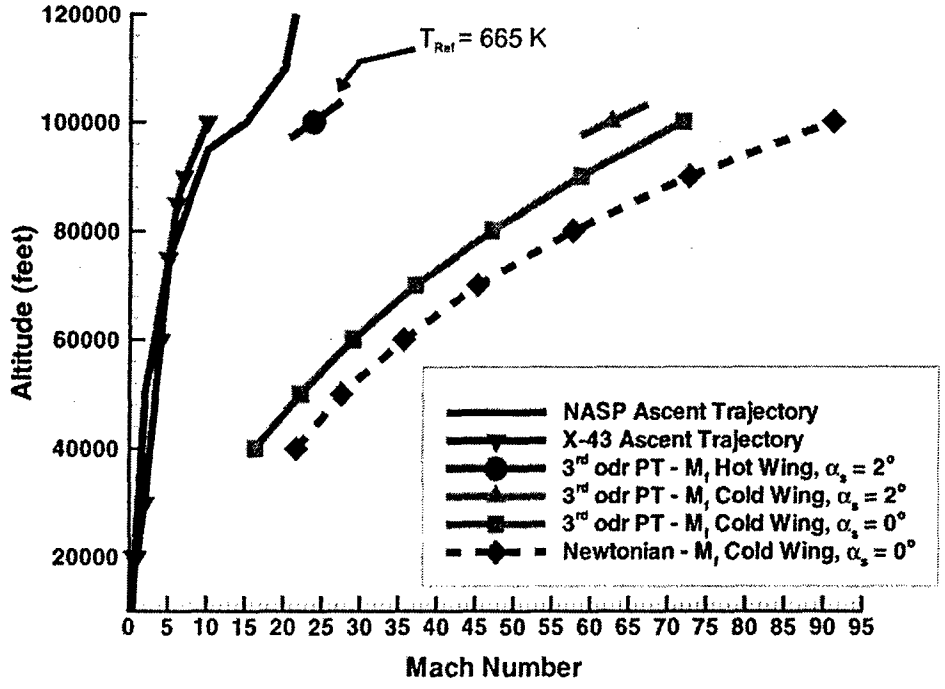

Figure 13: Comparison of flutter boundaries for modified low aspect ratio wing for ascent trajectories of typical hypersonic aircraft; flutter boundary for the heated wing at a 2 degree angle of attack corresponds to T_{Ref} =665 K

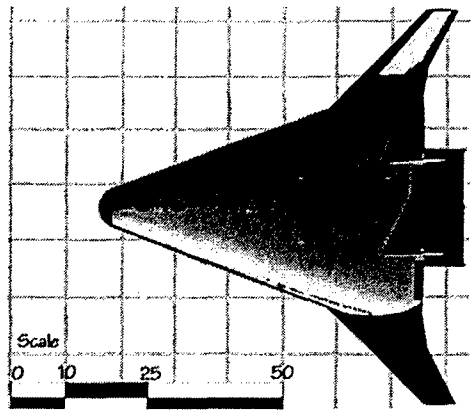

(a) X33, top view.

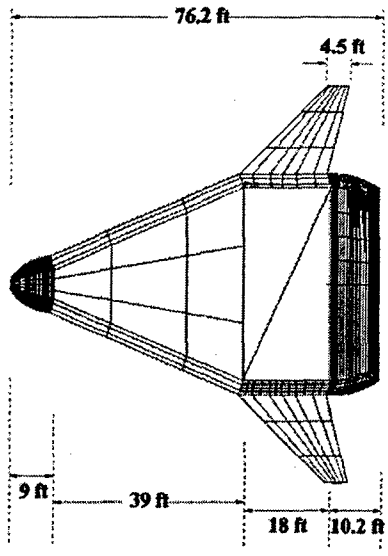

(b) Generic vehicle, top view.

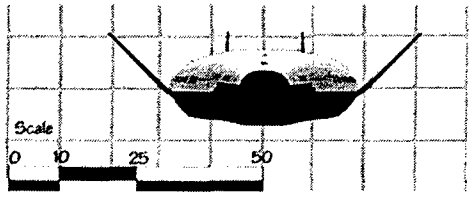

(c) X33, front view.

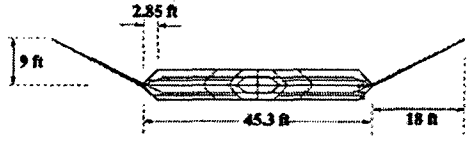

(d) Generic vehicle, front view.

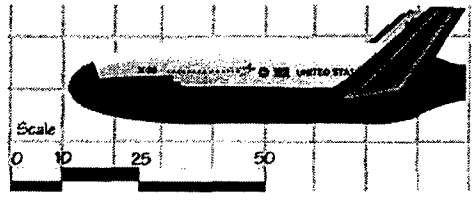

(e) X33, side view.

(f) Generic vehicle, side view.

Figure 14: X-33 and generic reusable launch vehicle.

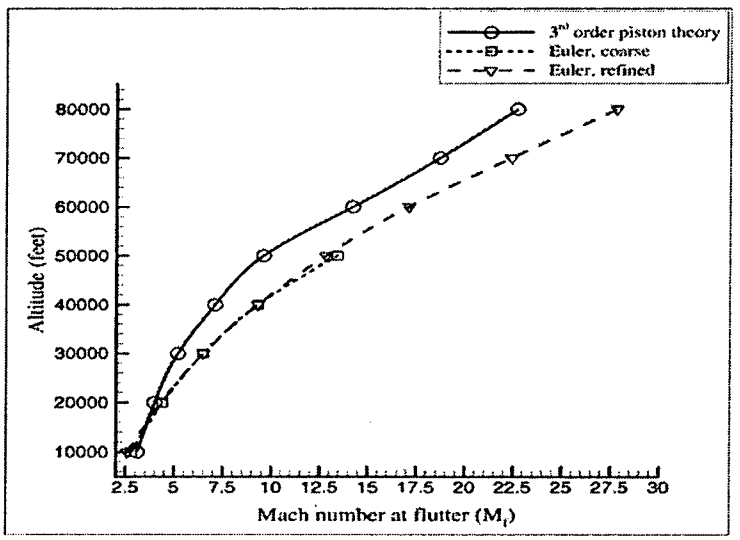

Figure 15: Flutter envelope of the generic hypersonic vehicle, calculated using 3rd order piston theory and Euler aerodynamics

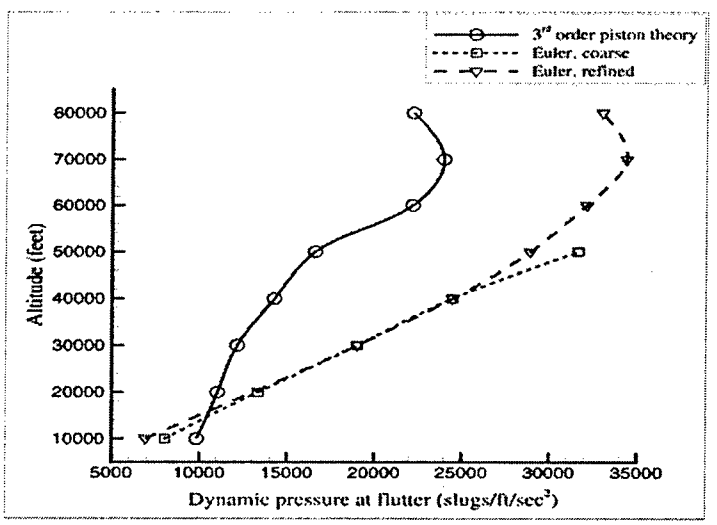

Figure 16: Dynamic pressure at flutter boundary for generic hypersonic vehicle, calculated using 3rd order piston theory and Euler aerodynamics

AFRL-SR-AR-TR-05-

0227

REPORT DOCUMENTATION PAGE

1. REPORT DATE: *25 May 2005*	2. REPORT TYPE -Final	3. DATES COVERED *Feb 1, 2001-Dec 31, 2004*

4. TITLE AND SUBTITLE

Aeroelasticity, Aerothermoelasticity and Aeroelastic Scaling of Hypersonic Vehicles

5a. CONTRACT NUMBER

5b. GRANT NUMBER
F49620-01-1-0158

5c. PROGRAM ELEMENT NUMBER

6. AUTHOR(S)

Peretz P. Friedmann

5d. PROJECT NUMBER

5e. TASK NUMBER

5f. WORK UNIT NUMBER

7. PERFORMING ORGANIZATION NAME(S) AND ADDRESS(ES)

University of Michigan
Department of Aerospace Engineering
1320 Beal Ave.
Ann Arbor, MI 48109-2140

8. PERFORMING ORGANIZATION REPORT NUMBER

9. SPONSORING / MONITORING AGENCY NAME(S) AND ADDRESS(ES)
Air Force Office of Scientific Research
4015 Wilson Blvd., Room 828-A
Arlington, VA 22203-1954

10. SPONSOR/MONITOR'S ACRONYM(S)

11. SPONSOR/MONITOR'S REPORT NUMBER(S)

12. DISTRIBUTION / AVAILABILITY STATEMENT

Approved for public release, distribution unlimited

13. SUPPLEMENTARY NOTES

14. ABSTRACT

This final report describes the work done during the period of the grant. Three separate hypersonic aeroelastic stability problems were considered: (a) a typical cross section having a double wedge airfoil, (b) the stability of a low aspect ratio wing, also with a double wedge airfoil, and (c) the behavior of a complete generic hypersonic vehicle. For problem (a) the unsteady airloads were computed using third order piston theory, as well as CFD based Euler and Navier-Stokes loads. For case (b) piston theory, Euler and Navier-Stokes based airloads were used, and case (c) both piston theory and Euler airloads were used. For the three –dimensional wing the treatment of thermal effect was also considered by solving the heat transfer problem using the Navier Stokes equations to determine the temperature distribution over the vehicle and conducting an aeroelastic analysis that accounts for the effect of thermal stresses and material degradation on the mode shapes. These mode shapes were used in an aeroelastic analysis based on 3rd order piston theory. This comprehensive treatment of the aerothermoelastic problem, the first of its kind in the literature, produces large reductions in aeroelastic stability margins. The results indicate that the flutter boundaries for third order piston theory can differ by 35% from those based on Euler unsteady loads. Solutions based on the loads obtained from the solution of the Navier-Stokes equation indicate further changes in aeroelastic stability margins. Important conclusions for the design of such vehicles are summarized in the body of the report.

15. SUBJECT TERMS

16. SECURITY CLASSIFICATION OF:			17. LIMITATION OF ABSTRACT	18. NUMBER OF PAGES	19a. NAME OF RESPONSIBLE PERSON
a. REPORT	b. ABSTRACT	c. THIS PAGE			Captain Clark Allred, Ph.D.
					19b. TELEPHONE NUMBER *(include area code)* 703-696-7259

Standard Form 298 (Rev. 8-98)
Prescribed by ANSI Std. Z39.18

6-21-05